

Naphthalocyanine-reconstituted LDL nanoparticles for *in vivo* cancer imaging and treatment

Liping Song^{1,2}

Hui Li²

Ulas Sunar³

Juan Chen^{2,4}

Ian Corbin^{2,4}

Arjun G Yodh³

Gang Zheng^{2,4}

¹Department of Chemistry, Shanghai University, China; ²Department of Radiology and ³Department of Physics and Astronomy, University of Pennsylvania, USA; ⁴Department of Medical Biophysics, University of Toronto, Ontario, Canada; Division of Biophysics and Bioimaging, Ontario Cancer Institute, Canada

Abstract: Low density lipoproteins (LDLs) are naturally occurring nanoparticles that are biocompatible, biodegradable and non-immunogenic. Moreover, the size of LDL particle is precisely controlled (~22 nm) by its apoB-100 component, setting them apart from liposomes and lipid micelles. LDL particles have long been proposed as a nanocarrier for targeted delivery of diagnostics and therapeutics to LDL receptor (LDLR)-positive cancers. Here, we report the design and synthesis of a novel naphthalocyanine (Nc)-based photodynamic therapy (PDT) agent, SiNcBOA, and describe its efficient reconstitution into LDL core (100:1 payload). Possessing a near-infrared (NIR) absorption wavelength (>800 nm) and extremely high extinction coefficient (>10⁵ M⁻¹cm⁻¹), SiNcBOA holds the promise of treating deeply seated tumors. Reconstituted LDL particles (r-Nc-LDL) maintain the size and shape of native LDL as determined by transmission electron microscopy, and also retain their LDLR-mediated uptake by cancer cells as demonstrated by confocal microscopy. Its preferential uptake by tumor *vs* normal tissue was confirmed *in vivo* by noninvasive optical imaging technique, demonstrating the feasibility of using this nanoparticle for NIR imaging-guided PDT of cancer.

Keywords: naphthalocyanine, lipoproteins, photodynamic therapy, near-infrared optical imaging, nanoparticle, drug delivery

Introduction

Nanoscale delivery systems engineered to home to cell surface receptors overexpressed in specific malignancies hold great promise to improve our ability to treat an ever-widening range of cancers (Sullivan and Ferrari 2004). These carriers are often superior to drug- or toxin-conjugated antibodies or ligands due to their ability to deliver high payload drugs per receptor recognition and to integrate multiple functions (eg, image-guided therapy) (Ferrari 2005). However many of these nanocarriers suffer from a number of shortcomings, thus limiting their clinical potential. For instance, a great deal of efforts has been invested in addressing synthetic nanoparticles' biocompatibility and toxicity issues, whereas lipid-based nanocarriers often lacks exquisite size control that may impact their reproducibility. Low-density lipoprotein (LDL) is the principal carrier of cholesterol in human plasma and delivers exogenous cholesterol to cells by endocytosis via the LDL receptor (LDLR) (Brown and Goldstein 1986). As an extraordinary high capacity (each native LDL can carry maximum 1500 cholesterol esters) and endogenous carrier, it is biocompatible, biodegradable and nonimmunogenic (Rensen et al 2001). In addition, the size of the LDL particle is precisely controlled (~22 nm) by its apoB-100 component through a network of amphipathic α -helix protein-lipid interactions (Lund-Katz et al 1998), setting it apart from liposomes and other lipid emulsions.

Correspondence: Gang Zheng
Ontario Cancer Institute/University
of Toronto, MaRS Center, TMDT
5-363, 101 College Street, Toronto,
Ontario M5G 1L7, Canada
Tel +1 416 581 7666
Fax +1 416 581 7667
Email gang.zheng@uhnres.utoronto.ca

The potential use of LDL as nanocarriers for targeted delivery of diagnostic and therapeutic agents to tumor cells has long been recognized (Krieger et al 1979; Gal et al 1981). Early observations identified that several hydrophobic drugs passively associate with plasma lipoproteins (Chassany et al 1994). In addition, drug-lipoprotein complexes were shown to have favorable pharmacologic profiles for drug delivery (Rudling et al 1983). Thereafter several independent laboratories demonstrated that various cytotoxic agents could be actively incorporated into lipoproteins (namely LDL) via intercalation or reconstitution methods (Firestone et al 1984; Masquelier et al 1986; Lundberg 1987; Samadi-Baboli et al 1990). Moreover these novel LDL-drug complexes were shown to be more efficacious against carcinoma cells than their conventional counterparts (Kader and Pater 2002). Experimentalists in the field of nuclear medicine were the first to demonstrate the utility of contrast agent conjugated LDL for imaging (Vallabhajosula et al 1988; Hay et al 1991). Radionuclides attached to apoB-100 or intercalated via amphiphilic chelates into LDL phospholipid monolayer were shown to be viable tracers for LDLR activity (Lees and Lees 1991; Jasanada et al 1996). Later the incorporation of near-infrared (NIR) fluorescent probes into LDL showed promise for optical imaging (Zheng et al 2002; Li et al 2004) and more recently gadolinium based agents have been attached to LDL for improved detection of tumors using magnetic resonance imaging (MRI) (Corbin et al 2006). The rationale for using LDL is based on the observation that many tumors actively take up LDL through the LDLR pathway (Hynds et al 1984; Vitols et al 1992; Caruso et al 2001). Up-regulated expression of LDLR in these cancer cells is thought to provide the substrates (cholesterol and fatty acids) needed for active membrane synthesis (Favre 1992). Recently, we developed a novel LDL rerouting technique to allow LDL to target any receptor of choice, thus expanding the utility of LDL nanocarriers far beyond the LDLR-positive tumors (Zheng et al 2005).

In this report, we describe the design and synthesis of a novel naphthalocyanine (Nc)-based photosensitizer (PS) as a suitable functional payload to be delivered by LDL nanoparticles for photodynamic therapy (PDT) (Dougherty et al 1998). The reason to select Nc-based PS as PDT agent is described as follows: (1) Nc is a neutral, porphyrin-like compound, that is much more stable photochemically and photophysically than corresponding porphyrin analogs (Ali and van Lier 1999). (2) Nc has photophysical properties consistent with its being an effective photosensitizer for PDT (Ali and van Lier 1999). Its 800 nm wavelength absorption

makes Nc ideal for applications where deep tissue penetration is important (Weissleder and Ntziachristos 2003) and its optical absorbance is extremely high ($\epsilon > 10^5 \text{ M}^{-1}\text{cm}^{-1}$) at this light wavelength. In addition, Nc is more intense and more red-shifted than Photofrin[®] at its optimal therapeutic wavelength (630 nm). Nc also exceeds most second generation PDT agents at its λ_{max} values (eg, Verteporfin[®] at 689 nm) (Dougherty et al 1998). Therefore, if the Nc-based PS can be reconstituted in LDL particles and be selectively delivered into tumor cells by LDLR, a tumor-targeted and NIR imaging-guided PDT treatment of deeply seated tumors can be achieved.

Here, we report the design and synthesis of tetra-*t*-butyl silicon naphthalocyanine bisoleate (SiNcBOA) suitable for LDL reconstitution. This report also describes the preparation and characterization of the Nc reconstituted LDL nanoparticles (r-Nc-LDL) (see Figure 1) as well as the *in vitro* and *in vivo* validation of the LDLR-targeting of this r-Nc-LDL to cancer cells and in mice bearing human hepatoblastoma G₂ (HepG₂) tumors.

Methods and materials

Materials

UV-vis spectra were recorded on a Perkin Lambda spectrophotometer (Boston, MA, USA). ¹H NMR and ¹³C NMR spectra were recorded on Bruker ASPECT 360 MHz instrument (Bruker, Billerica, MA, USA). Mass spectrometry analysis and elemental analysis were performed at the Mass Spectrometry Facility of the Department of Chemistry, University of Pennsylvania. All chemicals were purchased from Sigma-Aldrich (St. Louis, MO, USA) and all solvents were dried and redistilled before use. For TLC (Thin Layer Chromatography), EM Science TLC plates (silica gel 60 F₂₅₄) were used.

6-*tert*-butyl-2,3-dihydro-1,3-diimino-1H-benz[*f*]isoindole

Anhydrous NH₃ was slowly bubbled through a stirred mixture of 6-*tert*-butyl-2,3-naphthalenedicarbonitrile (4.0 g, 17.1 mmol) in NaOMe-MeOH solution (200 ml, 0.7 g Na in 200 ml MeOH) for 2 h. As NH₃ was introduced, the reaction mixture was refluxed for 3 h. After cooling, a portion of solvent was removed under reduced pressure. The resulting mixture stood for a while to form a yellow solid. The product was collected by filtration. The filtrate was poured into 200 mL of water with vigorous stirring. Thereafter, re-precipitation was performed to obtain more of the desired product, a yellow sticky solid. The total product obtained

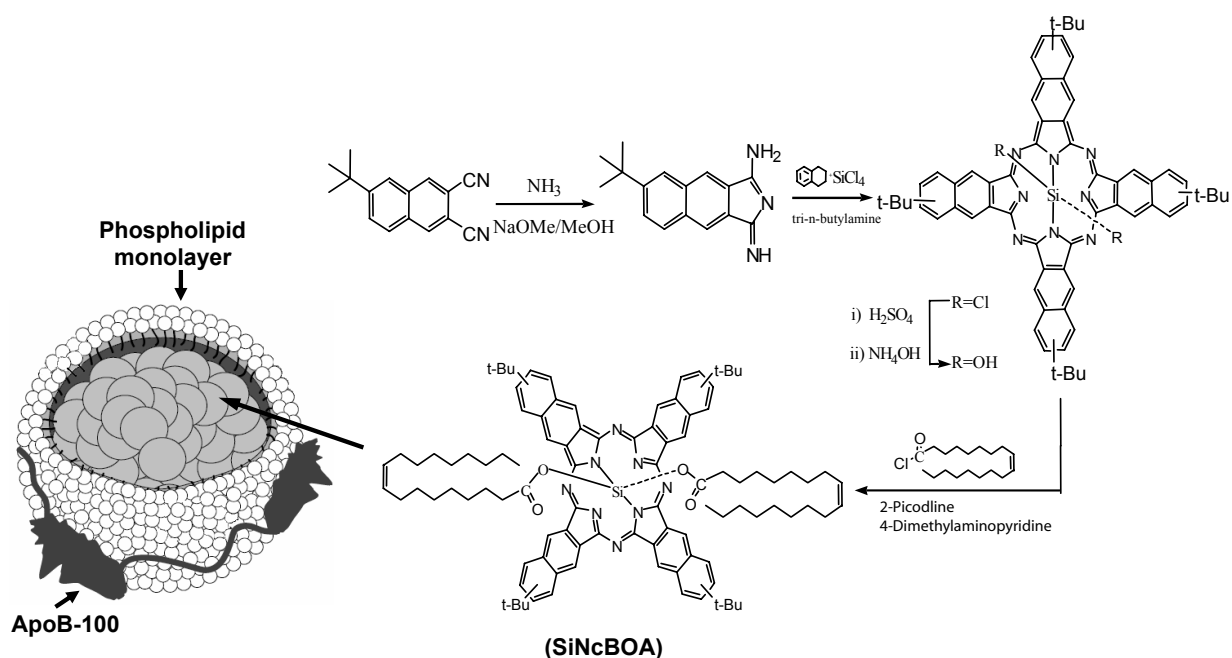


Figure 1 Synthesis of SiNcBOA and SiNcBOA-reconstituted LDL nanoparticles.

after washing and drying was 3.8 g (yield: 89%). This compound was used directly without further purification.

SiNcCl₂

A mixture of 6-*tert*-butyl-2,3-dihydro-1,3-diimino-1*H*-benz[*f*]isoindole (3.2 g, 12.8 mmol), SiCl₄ (2 mL, 17.5 mmol), dry tetrahydronaphthalene (20 mL), and dry tri-*n*-butylamine (15 mL) was refluxed for 2.5 h. The mixture was allowed to cool and diluted with methanol (25 mL). The product was filtered, washed with MeOH, and dried by air to acquire 1.675 g green solid SiNcCl₂ (yield: 51%). ¹H NMR; δ_H (500 MHz; CDCl₃) 1.46 (36 H, s) and 7.66–8.58 (20 H, m); ESI-MS. Calcd. for C₆₄H₅₆Cl₂N₈Si 1034.4 found by ESI-MS; 1035.1 (M+H)⁺.

SiNc(OH)₂

A mixture of crude SiNcCl₂ (700 mg, 0.68 mmol) and concentrated H₂SO₄ (22 mL) was stirred for 2 h and then poured over ice (40 g). The solid was filtered, washed with water, and resuspended in acetone and concentrated in NH₄OH (18 mL) to reflux for 2 h. After cooling, the resulting solid was filtered off and dried in high vacuum to acquire 610 mg of SiNc(OH)₂ (yield: 90 %). The product was dark-green.

Oleoyl chloride

The mixture of 1 g oleic acid (3.5 mmol), 5 mL CH₂Cl₂, 1 mL SOCl₂ and one drop of DMF were stirred at 40 °C for 12 h

under argon. The CH₂Cl₂ and excess SOCl₂ were removed afterwards under reduced pressure to acquire yellow sticky oil (oleoyl chloride) which was directly used for next step reaction without further purification.

SiNcBOA

To the flask of freshly prepared oleoyl chloride, 150 mg (0.15 mmol) of SiNc(OH)₂ and 20 mL 2-picoline were added. The suspension was stirred under nitrogen for 2 h. A portion of 4-dimethylaminopyridine (DMAP, 250 mg) was added to the mixture, which was then stirred under nitrogen for an additional 48 h at 60 °C. The solvent was removed under reduced pressure, and the product was purified by column chromatography (silica gel, CH₂Cl₂/hexane = 4/6 (V/V)) to yield dark green solid, 190 mg (83%) of SiNcBOA. ¹H NMR (300 MHz; CDCl₃): δ 9.97–9.81(m, 8H), 8.85–8.44 (m 8H), 8.05–8.03 (m, 4H), 5.25–5.09 (m, 4H), 1.92–1.85 (m, 4H), 1.74–1.69 (m, 36H, *t*-Bu), 1.65–1.60 (m, 4H), 1.27–1.20 (m, 24H), 0.90–0.80 (m, 8H), 0.78–0.74 (m, 4H), 0.57–0.48 (m, 4H), 0.27–0.10 (m, 4H), –0.01 –0.10 (m, 4H), –0.37 –0.51 (m, 6H). Elemental analysis calcd. for C₁₀₀H₁₂₂N₈O₄Si: C: 78.60, H: 8.05, N: 7.33; found: C: 78.77, H: 8.35, N: 6.85.

Preparation and characterization of r-Nc-LDL

LDL, purchased from Dr. Lund-Katz' lab at the Children's Hospital of Philadelphia (Philadelphia, PA), was isolated

from the fresh plasma of healthy donors by sequential ultracentrifugation as described previously (Lund-Katz et al 1998). LDL reconstitution with SiNcBOA was performed following a minor modification of the method of Krieger (Krieger 1986) Briefly, LDL (1.9 mg) was lyophilized with 25 mg starch, and then extracted three times with 5 mL of heptane at -5°C . Following aspiration of the last heptane extract, 6 mg of SiNcBOA was added in 200 μL of benzene. After 90 min at 4°C , benzene and any residual heptane were removed under a stream of N_2 in an ice salt bath for about 45 min. The r-Nc-LDL was solubilized in 10 mM Tricine, pH 8.2, at 4°C for 24 h. Starch was removed from the solution by a low-speed centrifugation ($500 \times g$) followed by a 20 min centrifugation ($6000 \times g$). The reconstituted LDL was stored under an inert gas at 4°C . Similarly, r-Nc-AcLDL was also prepared from SiNcBOA and acetylated LDL (AcLDL, Biomedical Technologies, Inc.) to be used as a control. The protein content of the specimen was determined by the Lowry method (Lowry et al 1951). The absorption spectrum of SiNcBOA was measured after extraction with a chloroform and methanol mixture (2:1), and probe concentration was calculated based on the following formula: $C = (A/\epsilon) \times D$, where C is the concentration of the probe, A is the O.D. value, ϵ is the extinction coefficient, and D is the dilution fold. Probe/protein molar ratio was calculated using the molecular mass of the ApoB-100 protein (514 kDa) knowing that one LDL particle contains only one ApoB-100.

Electron microscopy studies

Five microliters of the reconstituted LDL suspension was placed on carbon-coated 200 mesh copper grids and allowed to stand for 5 min. Excess sample was wicked off with lens paper and 2% Saturated Aqueous Uranyl Acetate was applied to the grid in 5 consecutive drops within 20 seconds. The stain was then drained off with filter paper and the grid was air dried. Digital images were taken using JEOL JEM 1010 electron microscope at 80 kv using AMT 12-HR software aided by Hamamatsu CCD Camera. All related supplies were purchased at Electron Microscopy Sciences (Fort Washington, PA, USA).

Cell preparations

LDLR overexpressing HepG₂ tumor cells, obtained from Dr. Theo van Berkel's laboratory from the University of Leiden in the Netherlands, were cultured in Dulbecco's modified Eagle's medium (DMEM) supplemented with 10% fetal bovine serum (FBS), 2 mM L-glutamine, 10 mM HEPES, 100 U/mL penicillin G sodium and 100 $\mu\text{g}/\text{mL}$

streptomycin sulfate. IdlA(mSR-BI) cells lacking LDLR, which were obtained from Dr. Monty Krieger (Massachusetts Institute of Technology, Cambridge, MA), were cultured in F-12K medium (Ham's Nutrient Mixture) with 2 mM L-glutamine, 100U/mL penicillin G sodium, 100 $\mu\text{g}/\text{mL}$ streptomycin sulfate, 300 $\mu\text{g}/\text{mL}$ active G418 and 5% FBS. All cells were grown at 37°C in a humidified atmosphere containing 5% CO_2 . HepG₂ cells (10×10^6) were inoculated subcutaneously into the right flanks of nude mice. The protocol was approved by the University of Pennsylvania Animal Ethics Committee.

Confocal microscopy studies

For confocal microscopy studies, HepG₂ and IdlA(mSR-BI) cells were grown in 4-well Lab-Tek chamber slides (Naperville, Illinois), respectively, at a density of 40,000 cells/well. Experiments were started, after two quick washes with pre-incubation medium (medium with 0.8% (w/v) BSA instead of FBS), by the addition of pre-incubation medium containing the indicated amounts of r-Nc-LDL. After 4 h incubation at 37°C , the cells were washed three times with ice-cold PBS and fixed for 15 minutes with 1% formaldehyde in PBS at room temperature. Then the chamber slides were mounted and sealed for confocal microscopy analysis. Confocal microscopy was performed on a Leica TCS SPII laser scanning confocal microscope (Heidelberg, Germany). Filter settings were 633 nm for excitation and 650–800 nm for emission.

In vivo tumor uptake of r-Nc-LDL monitored by Two-Channel I&Q Spectrometer

In vivo tumor absorption of r-Nc-LDL (140 μM , 200 μL , i.v.) by LDLR overexpressing HepG₂ tumor was measured using a two channel I&Q spectrometer (Sunar et al 2006). Acetylated LDL reconstituted with Nc (r-Nc-AcLDL) (628 μM , 50 μL , i.v.) was used as the negative control to further confirm the selective uptake of probe by tumor tissue. A brief description of I&Q spectrometer is as follows: A single 70 MHz radiofrequency signal from a generator is split into two parts. One signal is directed to the laser diode driver to amplitude modulate the source light intensity at 785 nm, and the other part is used as a reference. The intensity-modulated light is delivered to the tissue and the diffuse light is collected by 3 mm diameter avalanche photo-detectors. The output signals are amplified and band-pass filtered. The resulting signal is directed to IQ demodulators to derive the amplitude and phase of the signal. After low pass filtering, and converting

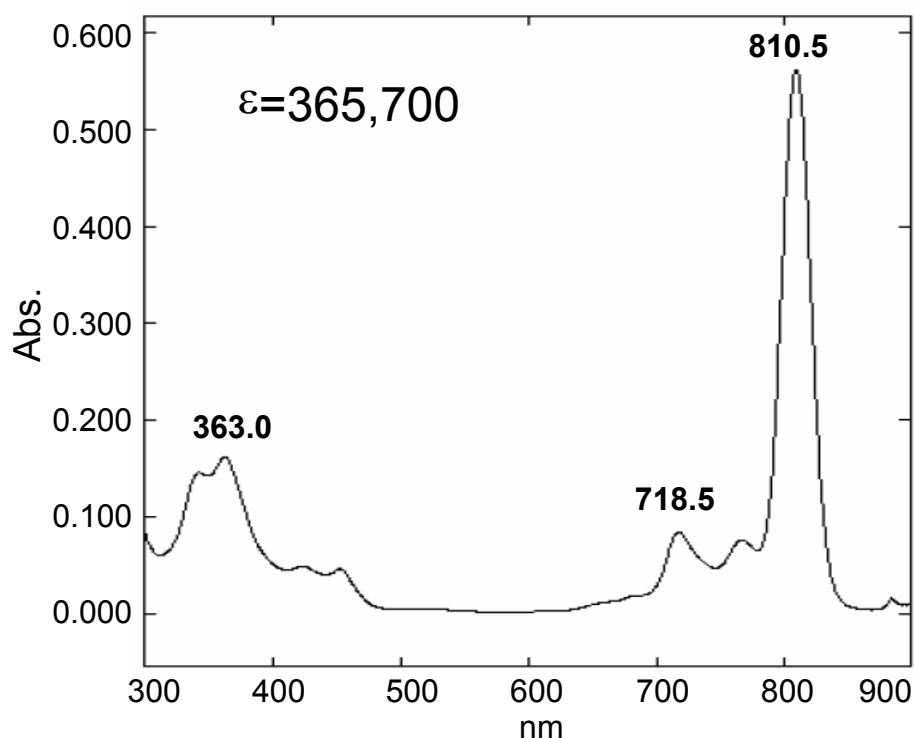


Figure 2 UV-vis spectrum of SiNcBOA.

signal from analog to digital, the data is collected by a laptop for post-processing.

Results and discussion

Design and synthesis of SiNcBOA

In order to achieve a sufficient payload of LDL-based naphthalocyanine for direct targeting of PS to LDLR, a neutral and hydrophobic SiNcBOA, tetra-*t*-butyl silicon naphthalocyanine bisoleate, was designed for LDL reconstitution. The Si coordination allows the binding of two axial oleate ligands (Li et al 2005), whereas the bulky *t*-butyl groups at the peripheral position of the Nc macrocycle increases the lipophilicity of this agent, allowing for better LDL reconstitution efficiency. In addition, these ligands anchor the dye into the LDL phospholipid monolayer, thus preventing the dissociation of the dye from LDL. Moreover, the steric hindrance created by these ligands on each side of the Nc ring limits the stack aggregation usually encountered in solution for these porphyrin-like planar molecular structures. This stacking phenomenon is responsible for the decreased triplet lifetime and cytotoxic singlet oxygen production of such PS. Therefore, using this novel SiNcBOA, we anticipate a high and efficient loading of this PS into LDL core.

The SiNcBOA was synthesized according to the protocol shown in Figure 1. The structure of SiNcBOA was confirmed

by ^1H NMR and elemental analysis and its absorption spectra showed an intense absorption at 810 nm with extinction coefficient $\epsilon = 3.7 \times 10^5$ (Figure 2). This extremely high absorption in NIR wavelength range is ideal for treating deeply seated tumors, since NIR excitation light has a large tissue penetration (Weissleder et al 2003).

LDL nanoparticle preparation and characterization

r-Nc-LDL was prepared by reconstituting SiNcBOA into LDL lipid core. The success of the reconstitution was evaluated by measuring the protein recovery (= protein content of r-Nc-LDL / protein content of total LDL for reconstitution). Forty-five to sixty percent protein recovery was observed for SiNcBOA reconstituted LDL particle (r-Nc-LDL). Given that the UV spectrum of SiNcBOA is the same both before and after LDL reconstitution, the absorbance at 810 nm was used to calculate the SiNcBOA concentration in the reconstituted LDL. It was found that approximately 100 SiNcBOA molecules were reconstituted into each LDL nanoparticle.

The size of r-Nc-LDL was directly measured by electron microscopy. As shown in Figure 3, the mean particle size of r-Nc-LDL was 21.1 ± 3.4 nm ($n = 25$), this is about the same size as native LDL (20 ± 2.7 nm, $n = 37$). These findings

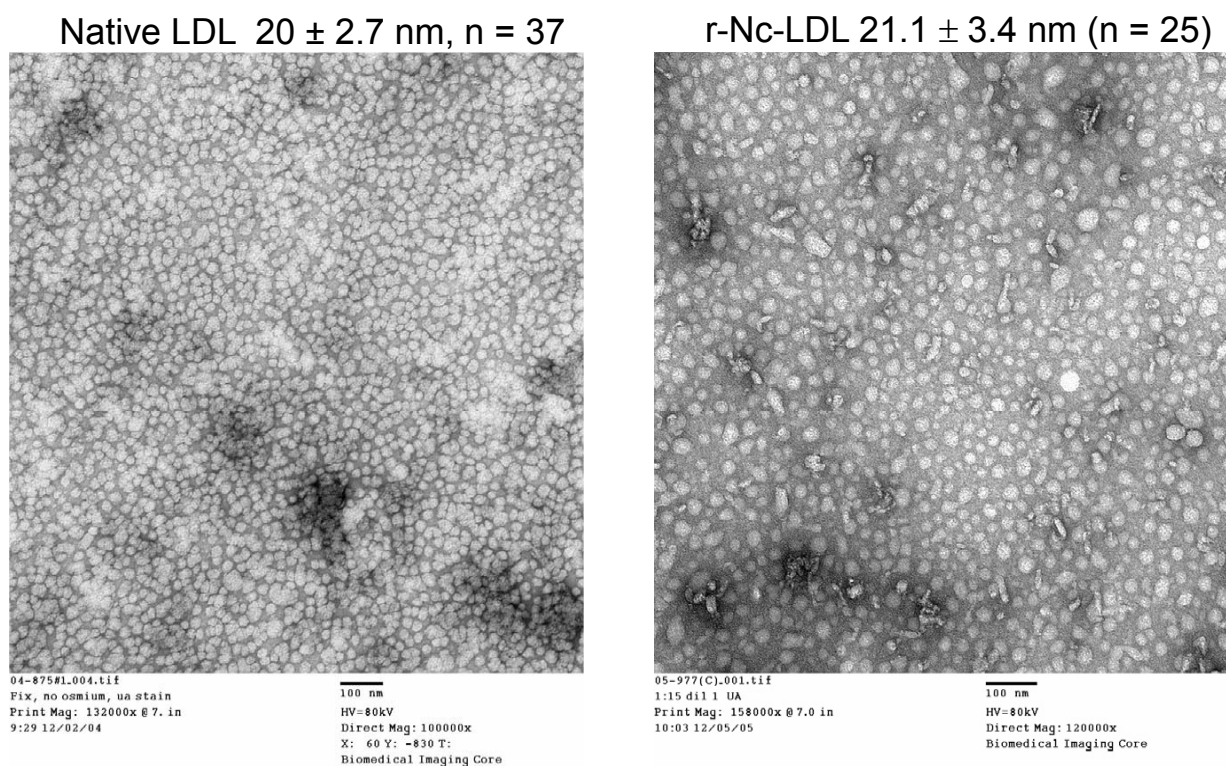


Figure 3 EM images of native LDL (left) and r-Nc-LDL (right) nanoparticles.

indicate that reconstitution of SiNcBOA into LDL did not change the size of the LDL particle.

In vitro validation of the LDLR-specific uptake of r-Nc-LDL

To evaluate the LDLR mediated cell uptake of r-Nc-LDL, a confocal microscopy study was performed on LDLR over-expressing HepG₂ cells (LDLR⁺) and LDLR less-expressing Id1A(mSR-BI) cells (LDLR⁻) (Figure 4). Although the confocal laser setting (Ex. 633nm, Em: >650 nm) is not optimal for visualizing SiNcBOA fluorescence, accumulation of r-Nc-LDL into HepG₂ (LDLR⁺) cells was evident and this accumulation was concentration dependent (Figure 4B, 4C). The LDLR specific uptake of r-Nc-LDL is supported by the following experiments: 1) 25-fold excess of native LDL completely blocked the uptake of r-Nc-LDL by HepG₂ Cells (LDLR⁺) (Figure 4D), 2) uptake of r-Nc-LDL into Id1A(mSR-BI) (LDLR⁻) cells was not observed even at higher LDL nanoparticle concentration (Figure 4F). Taken together, these results indicate that r-Nc-LDL was internalized into HepG₂ cells specifically via the LDLR mediated pathway.

In vivo validation of LDLR-specific accumulation of r-Nc-LDL

In order to validate the LDLR mediated uptake of r-Nc-LDL in vivo, a negative control was prepared by reconstituting

SiNcBOA into AcLDL (r-Nc-AcLDL). The acetylated Lys residues of AcLDL prevent it from binding to LDLR, thus AcLDL serves as a valid negative control.

The two-channel I&Q spectrometer was used for in vivo monitoring the r-Nc-LDL nanoparticle accumulation in HepG₂ tumors. As showed in Figure 5, significant absorption enhancement was observed in tumor tissue compared to the surrounding muscle tissue after intravenous injection of the nanoparticle. The tumor to normal muscle ratio reached a maximum of 8:1 at 2 h post-injection. Conversely, injection of r-Nc-AcLDL into tumor-bearing mice did not result in absorption enhancement in either tumor or host muscle tissues. These findings independently validate the in vivo LDLR-mediated uptake of r-Nc-LDL into HepG₂ tumors.

Conclusions

The near infrared optical imaging/PDT agent, SiNcBOA, was synthesized and successfully reconstituted into LDL lipid core at a high payload. The LDLR targeted tumor uptake of this dual probe was demonstrated both in vitro by confocal microscopy and in vivo by I&Q spectrometry. The data demonstrates that r-Nc-LDL is an efficacious NIR optical contrast agent with a high absorption $\epsilon = 3.7 \times 10^5$ at 810 nm. The PDT efficacy of this agent is currently under the investigation. Potentially, this biocompatible r-Nc-LDL nanoparticle offers

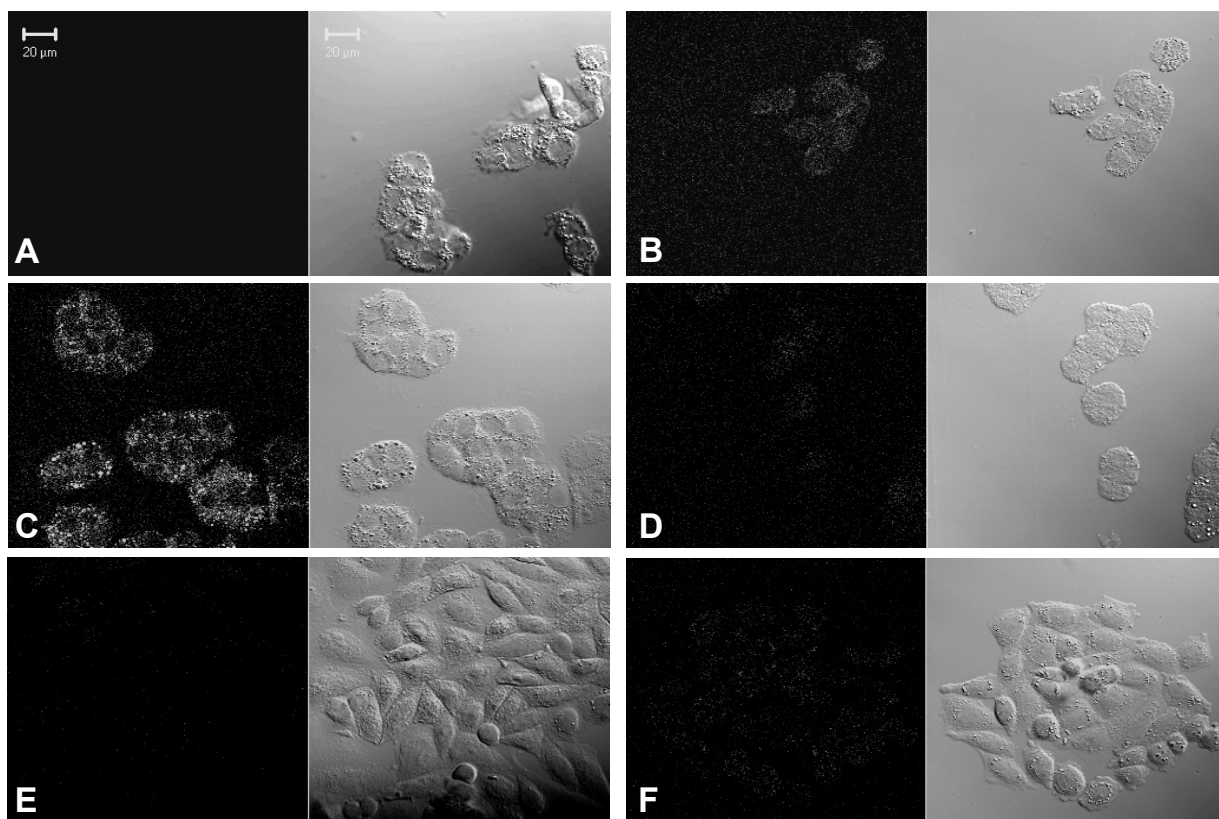


Figure 4 Confocal images of: **(A)** HepG₂ cells alone (LDLR⁻), **(B)** HepG₂ + 50 μM of r-Nc-LDL, **(C)** HepG₂ + 200 μM of r-Nc-LDL, **(D)** HepG₂ + 50 μM of r-Nc-LDL + 25 fold excess native LDL, **(E)** IdIA(mSR-BI) cells alone (LDLR⁻), and **(F)** IdIA(mSR-BI) + 200 μM of r-Nc-LDL. The letters refer to each pair of images, with the fluorescence images on the left and the bright field images on the right.

the opportunity to noninvasively treat deeply-seated tumors with NIR imaging-guided PDT. Our laboratory has recently reported that by conjugating homing ligands onto the surface of ApoB-100, LDL can be re-directed to alternate cell surface receptors and epitopes (Zheng et al 2005), thus expanding

the opportunity for therapeutic applications of this r-Nc-LDL nanoparticle to a wider range of tumor types.

Note

Liping Song and Hui Li contributed equally to this work.

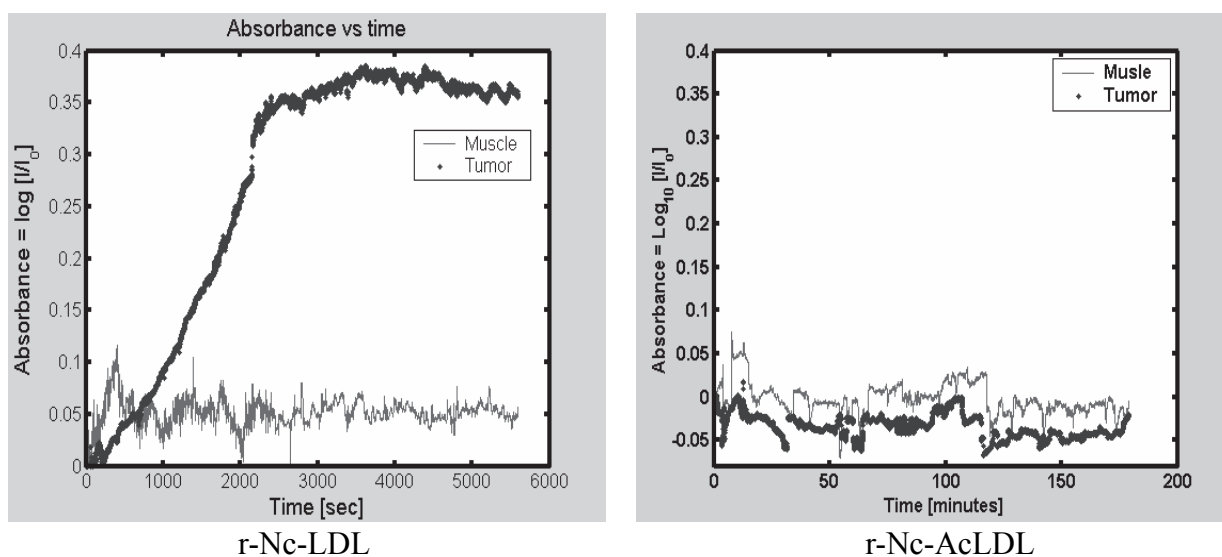


Figure 5 I & Q spectrum of HepG₂ tumor and normal muscle after r-Nc-LDL (left) or r-Nc-AcLDL (right) intravenous injection.

Acknowledgments

This work was supported by grants from NIH R21/R33 CA114463, CIHR 166453, the Radiological Society of North America (RSNA) and the Joey and Toby Tanenbaum/Brazilian Ball Chair in Prostate Cancer Research, Ontario Cancer Institute (GZ).

References

- Ali H, van Lier JE. 1999. Metal complexes as photo- and radiosensitizers. *Chem Rev*, 99:2379–450.
- Brown MS, Goldstein JL. 1986. A receptor-mediated pathway for cholesterol homeostasis. *Science*, 232:34–47.
- Caruso MG, Notarnicola M, Cavallini A, et al. 2001. Low density lipoprotein receptor and mRNA expression in human colorectal cancer. *Anticancer Res*, 21:429–33.
- Chassany O, Urien S, Claudepierre P, et al. 1994. Binding of anthracycline derivatives to human serum lipoproteins. *Anticancer Res*, 14:2353–5.
- Corbin IR, Li H, Chen J, et al. 2006. Low-density lipoprotein nanoparticles as magnetic resonance imaging contrast agents. *Neoplasia*, 8:488–98.
- Dougherty TJ, Gomer CJ, Henderson BW, et al. 1998. Photodynamic therapy. *J Natl Cancer Inst*, 90:889–905.
- Favre G. 1992. Targeting of tumor cells by low density lipoproteins: principle and use of ellipticin derivatives. *C R Seances Soc Biol Fil*, 186:73–87.
- Ferrari M. 2005. Cancer nanotechnology: opportunities and challenges. *Nat Rev Cancer*, 5:161–71.
- Firestone RA, Pisano JM, Falck JR, et al. 1984. Selective delivery of cytotoxic compounds to cells by the LDL pathway. *J Med Chem*, 27:1037–43.
- Gal D, Ohashi M, MacDonald PC, et al. 1981. Low-density lipoprotein as a potential vehicle for chemotherapeutic agents and radionuclides in the management of gynecologic neoplasms. *Am J Obstet Gynecol*, 139:877–85.
- Hay RV, Fleming RM, Ryan JW, et al. 1991. Nuclear imaging analysis of human low-density lipoprotein biodistribution in rabbits and monkeys. *J Nucl Med*, 32:1239–45.
- Hynds SA, Welsh J, Stewart JM, et al. 1984. Low-density lipoprotein metabolism in mice with soft tissue tumours. *Biochim Biophys Acta*, 795:589–95.
- Jasanada F, Urizzi P, Souchard JP, et al. 1996. Indium-111 labeling of low density lipoproteins with the DTPA-bis(stearylamide): evaluation as a potential radiopharmaceutical for tumor localization. *Bioconjug Chem*, 7:72–81.
- Kader A, Pater A. 2002. Loading anticancer drugs into HDL as well as LDL has little affect on properties of complexes and enhances cytotoxicity to human carcinoma cells. *J Control Release*, 80:29–44.
- Krieger M. 1986. Reconstitution of the hydrophobic core of low-density-lipoprotein. *Methods Enzymol*, 128:608–13.
- Krieger M, Smith LC, Anderson RG, et al. 1979. Reconstituted low density lipoprotein: a vehicle for the delivery of hydrophobic fluorescent probes to cells. *J Supramol Struct*, 10:467–78.
- Lees AM, Lees RS. 1991. 99mTechnetium-labeled low density lipoprotein: receptor recognition and intracellular sequestration of radiolabel. *J Lipid Res*, 32:1–8.
- Li H, Marotta DE, Kim S, et al. 2005. High payload delivery of optical imaging and photodynamic therapy agents to tumors using phthalocyanine-reconstituted low-density lipoprotein nanoparticles. *J Biomed Opt*, 10:41203.
- Li H, Zhang Z, Blessington D, et al. 2004. Carbocyanine labeled LDL for optical imaging of tumors. *Acad Radiol*, 11:669–77.
- Lowry OH, Rosebrough NJ, Farr AL, et al. 1951. Protein measurement with the Folin phenol reagent. *J Biol Chem*, 193:265–75.
- Lund-Katz S, Laplaud PM, Phillips MC, et al. 1998. Apolipoprotein B-100 conformation and particle surface charge in human LDL subspecies: implication for LDL receptor interaction. *Biochemistry*, 37:12867–74.
- Lundberg B. 1987. Preparation of drug-low density lipoprotein complexes for delivery of antitumoral drugs via the low density lipoprotein pathway. *Cancer Res*, 47:4105–8.
- Masquelier M, Vitols S, Peterson C. 1986. Low-density lipoprotein as a carrier of antitumoral drugs: in vivo fate of drug-human low-density lipoprotein complexes in mice. *Cancer Res*, 46:3842–7.
- Rensen PC, de Vruhe RL, Kuiper J, et al. 2001. Recombinant lipoproteins: lipoprotein-like lipid particles for drug targeting. *Adv Drug Deliv Rev*, 47:251–76.
- Rudling MJ, Collins VP, Peterson CO. 1983. Delivery of aclacinomycin A to human glioma cells in vitro by the low-density lipoprotein pathway. *Cancer Res*, 43:4600–5.
- Samadi-Baboli M, Favre G, Bernadou J, et al. 1990. Comparative study of the incorporation of ellipticine-esters into low density lipoprotein (LDL) and selective cell uptake of drug – LDL complex via the LDL receptor pathway in vitro. *Biochem Pharmacol*, 40:203–12.
- Sullivan DC, Ferrari M. 2004. Nanotechnology and tumor imaging: seizing an opportunity. *Mol Imaging*, 3:364–9.
- Sunar U, Quon H, Durduran T, et al. 2006. Noninvasive diffuse optical measurement of blood flow and blood oxygenation for monitoring radiation therapy in patients with head and neck tumors: a pilot study. *J Biomed Opt*, 11:064021.
- Vallabhajosula S, Paidi M, Badimon JJ, et al. 1988. Radiotracers for low density lipoprotein biodistribution studies in vivo: technetium-99m low density lipoprotein versus radioiodinated low density lipoprotein preparations. *J Nucl Med*, 29:1237–45.
- Vitols S, Peterson C, Larsson O, et al. 1992. Elevated uptake of low density lipoproteins by human lung cancer tissue in vivo. *Cancer Res*, 52:6244–7.
- Weissleder R, Ntziachristos V. 2003. Shedding light onto live molecular targets. *Nat Med*, 9:123–8.
- Zheng G, Chen J, Li H, et al. 2005. Rerouting lipoprotein nanoparticles to selected alternate receptors for the targeted delivery of cancer diagnostic and therapeutic agents. *Proc Natl Acad Sci U S A*, 102:17757–62.
- Zheng G, Li H, Yang K, et al. 2002. Tricarbocyanine cholesteryl laurates labeled LDL: new near infrared fluorescent probes (NIRFs) for monitoring tumors and gene therapy of familial hypercholesterolemia. *Bioorg Med Chem Lett*, 12:1485–8.